Eur. Phys. J. B **54**, 211–216 (2006)
DOI: 10.1140/epjb/e2006-00446-8

THE EUROPEAN PHYSICAL JOURNAL B

Atomic motion in Se nanoparticles embedded into a porous glass matrix

I.V. Golosovsky[1,a], O.P. Smirnov[1], R.G. Delaplane[2], A. Wannberg[2], Y.A. Kibalin[3], A.A. Naberezhnov[4], and S.B. Vakhrushev[4]

[1] Petersburg Nuclear Physics Institute, 188300, Gatchina, St. Petersburg, Russia
[2] Neutron Research Laboratory, Studsvik, 611 82 Nyköping, Sweden
[3] St. Petersburg State Polytechnical University, 195251, St. Petersburg, Russia
[4] A.F. Ioffe Physico-Technical Institute, 194021, St. Petersburg, Russia

Received 21 July 2006 / Received in final form 2 November 2006
Published online 22 December 2006 –

Abstract. By neutron diffraction it was shown that nanostructured Se confined within a porous glass matrix exists in a crystalline as well as in an amorphous state. The spontaneous crystallization of crystalline Se from confined amorphous phase was observed. The root-mean-square amplitudes of the atomic motions in the bulk as well as in confinement are found to be essentially different in a basal plane and in the perpendicular direction along the hexagonal axis. The atomic motions in the confined Se differ from the atomic motions in the bulk at low temperatures. The results shows an unusual "freezing" of the atomic motion along the chains, while the atomic motions in the perpendicular plane still keep. This "freezing" is accompanied by the deformation of nanoparticles and the appearance of inner stresses. This effect is attributed to the interaction of confined nanoparticle with the cavity walls.

PACS. 61.46.-w Nanoscale materials – 61.12.Ld neutron diffraction. – 63.22.+m Phonons or vibrational states in low-dimensional structures and nanoscale materials

1 Introduction

The thermal motions of atoms determine such fundamental properties of the solids as thermal-conductivity, thermal-expansion, heat capacity and melting-freezing transition. However, little is known about the atomic vibrations in nanoparticles, where the size of the system becomes comparable with the characteristic length of interatomic interactions and a wavelength of atomic vibration is limited by nanoparticle dimension.

In the case of "restricted geometry" when nanoparticles are confined within cavities of a porous media the interaction with cavity walls modifies the atomic motion. Therefore the spectrum of thermal vibrations of confined nanoparticles should be significantly changed because the amount of atoms located near to the surface is comparable with the total number of atoms in a nanoparticle.

In this context the behavior of the classic semiconductor selenium in confinement is especially interesting. This semi-metal is used in solar cells, light flux-meters, xerography and for other application.

In the crystalline state Se has several structure modifications [1]. However, under the normal conditions only the trigonal phase is stable; the others, being metastable, slowly convert to the trigonal form [2,3]. The crystal structure of trigonal Se consists of rigid spiral chains, which are weakly bonded in between (Fig. 1), while the structure of monoclinic form consists of eight-membered rings. Therefore crystalline Se easily transforms to the glassy amorphous state and conversely, keeping the the short fragments of spirals or the eight-membered rings as the structure units.

The thermal motion in the selenium nanoparticles crystallized within the amorphous Se by the melt quenching technique [4] has been investigated by X-ray diffraction in temperature range 88–325 K [5,6]. There are some reports on the Se embedded within various forms of zeolites. However super-small cage dimensions limit the size of the selenium entities and prevent Se crystallization [7–9]. Therefore the role of confinement in the thermal motion, especially at low temperatures remains still open.

In this paper we present the comparative neutron diffraction studies of the nanostructured Se within a porous vycor-glass matrix and the bulk Se in the temperature interval 4.2–500 K. Selenium was embedded into a porous matrix under applied pressure. This method allows to insert a significant amount of Se, that gives the possibility to use neutron diffraction.

The information about the temperature dependence of atomic motion in the bulk selenium is rather scarce and

[a] e-mail: golosov@mail.pnpi.spb.ru

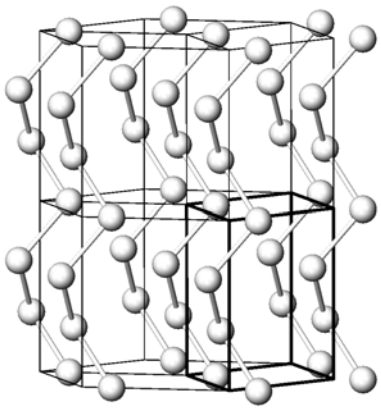

Fig. 1. Hexagonal crystal structure of Se. A unit cell is shown by the solid line. Hexagonal axis is directed vertically.

controversial. For example, the reported data on Debye temperature in the bulk Se at room temperature varies from 90 K [12] to 160 K [13]). Therefore for comparison we performed neutron diffraction experiments with the high purity bulk Se.

The neutron diffraction is a very powerful method for studies of thermal vibrations since it offers the direct measurement of the atomic displacements and has such advantage over X-ray diffraction as low absorption of neutrons, which practically does not affect the measured thermal parameters.

2 Experiment

Selenium was embedded in the porous matrix by a special technique under external pressure 10 Kbars in the molten state. After decreasing temperature it crystallizes within nanopores.

The silica matrix with the mean pore diameter 70(5) Å has a random interconnected network of elongated pores with a narrow distribution of the pore diameters [11]. In order to observe the dynamic properties of the embedded compounds at elevated temperatures such matrix is preferable because of its high thermo-resistance. Moreover the amorphous SiO_2 does not give any additional Bragg reflections in the diffraction pattern.

For experiments with the bulk to minimize the content of the amorphous Se, which usually co-exists with the crystalline phase the Se powder was annealed at about 200 °C for 24 h.

The neutron diffraction experiments have been performed with the diffractometer SLAD [14] of the Studsvik Neutron Research Laboratory at temperatures 15–493 K using a neutron wavelength of 1.118 Å. This diffractometer is not equipped with fine collimators, that leads to non-Gaussian instrumental lineshape, however provides high luminosity. Low temperature neutron diffraction studies of the bulk Se were carried out at the powder diffractometer of PNPI at a neutron wavelength of 1.36 Å. All diffraction patterns were analyzed with the FullProf program [15].

The intensity of the diffraction reflection is proportional to the square of the atomic temperature factor $T_k(\mathbf{Q})$, which in the approximation of the independent normal modes can be written as follows

$$T_k(\mathbf{Q}) = \exp\left(-\frac{1}{2}\langle(\mathbf{Q}\cdot\mathbf{u}_k)^2\rangle\right), \quad (1)$$

here $\mathbf{u}_k$ is the displacement of k-atom. Therefore from the reduction of the Bragg reflections with the transfer momentum $\mathbf{Q}$ one can get information about the atomic thermal vibrations.

In isotropic case the atomic motion is usually expressed by the isotropic Debye-Waller factor $B = 8\pi^2\langle u^2\rangle$. In this case the atomic temperature factor reduces to

$$T_{iso}(Q) = \exp\left(-B\frac{Q^2}{16\pi^2}\right). \quad (2)$$

In anisotropic case it is customary to describe the atomic displacements in the terms of anisotropic temperature parameters β_{ij}, which in fact are refined variables and related with the mean-square amplitudes of the atomic motion by the unitary transformation [16].

The absorption of neutrons with a wavelength of 1.118 Å in selenium is small and does not affect the measured Debye-Waller factors. Indeed, taking into account the absorption correction increases of the isotropic Debye-Waller factor for about 0.005 Å^2, which is negligible in comparison with the statistical error of about 0.1–0.05 Å^2.

3 Experimental results and discussion

3.1 Crystal structure of confined Se

All observed reflections from nanostructured Se were indexed in the trigonal space group $P3_121$. The presence of others modifications was not detected. The result of profile refinement of a typical neutron diffraction pattern is shown at Figure 2.

The observed peak broadening in comparison with the instrumental linewidth results from size-effect and/or inner stresses. However because of the different angle dependence these contributions can be easily separated. Using the Thompson-Cox-Hastings approximation of the lineshape with independent variation of the Gauss and Lorenz contributions [17] we found that the inner stresses appear only below about 100 K. Above this temperature the peak broadening results from a size-effect only. The volume averaged diameter of the confined nanoparticles was found to be of 183(6) Å. Starting from about 400 K the nanoparticle size increases drastically demonstrating the melting process.

The averaged diameter of the confined nanoparticles appears to be noticeably larger than the estimated mean diameter of a nanopore of 70(5) Å. This fact had been already marked for practically all compounds embedded in a porous glass (see for example Ref. [18]), and it was attributed to the spreading of crystallization process to the adjacent pores.

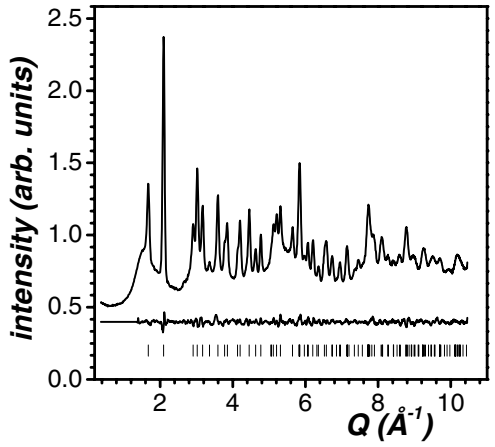

Fig. 2. Observed (at the top) and difference (at the bottom) neutron diffraction patterns of the nanostructured Se embedded in a porous glass at 300 K. Strong diffuse scattering origins mainly from amorphous porous glass. Vertical bars mark the reflection positions.

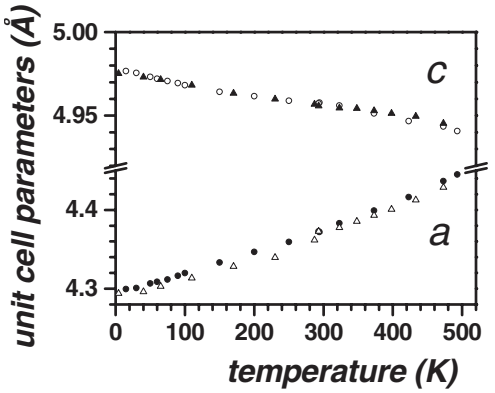

Fig. 3. Solid and open circles correspond to the unit cell parameters a (in the basal plane) and c (along the hexagonal axis) for the nanostructured Se while open and solid triangles correspond to those for the bulk.

The values and temperature behavior of the measured unit cell parameters was found to be similar to that observed for nanocrystalline Se synthesized by melt-quenching of amorphous Se [5,6] (Fig. 3). In this figure it is seen that the parameter a, basal edge of the hexagonal cell, is systematically smaller than that of the bulk. Structure positional parameter x, which defines the bonds and angles in Se chain along the hexagonal axis c, does not show any anomaly and linearly decreases with temperature increasing.

The hexagonal unit cell parameters of confined Se at room temperature $a = 4.3729(3)$ and $c = 4.9557(4)$ slightly differ from the reported single crystal unit cell parameters $a = 4.3662$ and $c = 4.9536$ [2]. Because of the strongly anisotropic shape of the unit cell it is natural to expect an anisotropic shape for embedded nanoparticles. Indeed, in the case of nanostructured Se synthesized by crystallization from amorphous Se the anisotropic shape of nanoparticles was observed experimentally [4]. Moreover,

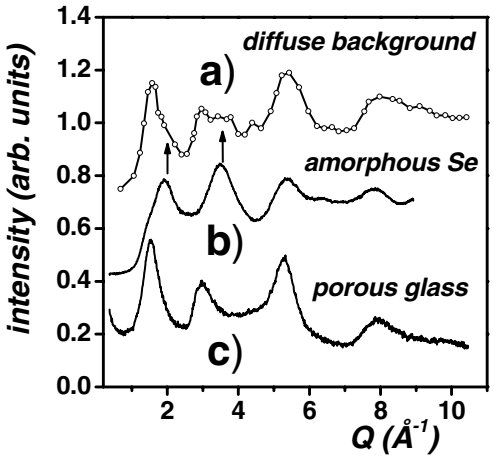

Fig. 4. (a) Diffuse background calculated by the interpolation of the points where the Bragg contribution is negligible; (b) Diffraction pattern of amorphous Se; (c) Diffraction pattern from unfilled porous glass.

in the recent neutron diffraction experiments with confined Pb we detected the anisotropic shape of nanoparticles too [10]. However, in the case of Se we did not succeed in finding any systematic broadening of the diffraction reflections beyond the limits of statistical accuracy.

3.2 High temperature crystallization of amorphous Se

In Figure 4a the diffuse background calculated by the interpolation of the points where the Bragg contribution is negligible is shown. It turns out that this profile does not coincide with the diffuse scattering profile measured from a pure porous matrix (Fig. 4c). However the positions of the additional peaks clearly seen at the background pattern (shown by the arrows in the figure) coincide with the peaks at the diffuse scattering pattern from the amorphous Se shown in Figure 4b [19]. This analysis evidences that Se presents in the matrix pores not only in a crystalline state but in an amorphous state as well.

With increasing temperature a part of the amorphous Se within pores starts to crystallize into the trigonal Se. In Figure 5 the temperature dependence of the scale factor, which is proportional to the amount of crystalline phase is shown. It is seen that the formation of the crystalline Se from the amorphous part starts at about 50 °C and undergoes a maximum at about 150 °C. After that the scale factor goes down because of the melting.

The coexistence of the crystalline and the amorphous Se is not surprising and can be explained by the phase instability of confined Se [9]. The co-existence of the disordered Se clusters and the trigonal crystalline Se had been observed within $AlPO_4$-5 zeolite voids by the Raman spectroscopy [8]. The reported transition temperature coincides with our observation, i.e. the phase transformation in confinement does not depend on matrix topology.

From the slope of the scale factor at the highest temperatures (Fig. 5) the melting point of confined Se can

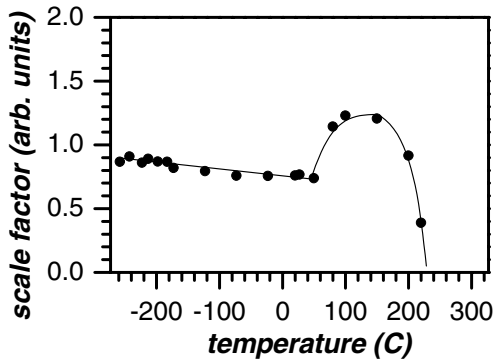

Fig. 5. Temperature dependence of the scale factor proportional to the amount of crystalline phase. The error is about the size of the symbols.

be estimated by the extrapolation to the temperature of 229(2) °C, while for the bulk the melting point is of 221 °C. In Figure 5 it is seen that at the last experimental point of 220(1) °C, the scale factor is well above the zero, i.e. the crystalline phase still exists. It evidences that the melting point, considered as the point when the melting is completed, in confinement is higher than in the bulk.

The increasing of the melting point in confinement has been observed for different confined compounds [20], in particular in Pb embedded in a porous glass [10], and is attributed to the specific peculiarity of the "restricted geometry" for the nanoparticles confined to irregular pores of SiO_2 matrix.

3.3 Atomic motion in confined Se

From the temperature dependence of the Bragg intensity the anisotropic β_{ij} factors and the root-mean-square (rms) amplitudes were calculated for the bulk and for confined Se. In Figure 6 the temperature dependences of the isotropic and anisotropic parts of the rms amplitudes are shown.

The observed temperature dependence of the isotropic part of the rms amplitude for the bulk shows a large static contribution at $T = 0$. Usually such static contribution is explained by the pinning the atomic motion by defects. The comparative data on the static and the temperature dependent part of the atomic motion are controversial [5]. However, in the studied case the static contribution in the isotropic rms amplitudes for confined nanoparticles and for the bulk appear to be very close. It means that the static term should be considered as intrinsic.

The fit of the temperature dependence of the isotropic part of the mean-square displacement for the bulk $\langle u^2 \rangle$ in the frame of the Debye theory [16]:

$$\langle u^2 \rangle = \frac{3\hbar^2 T}{m k_B {\Theta_D}^2} \left[F\left(\frac{\Theta_D}{T}\right) + \frac{\Theta_D}{4T} \right] \qquad (3)$$

where m, $\hbar$ and k_B, T — the atomic mass, the Planck and the Boltzmann constants, temperature, respectively, and

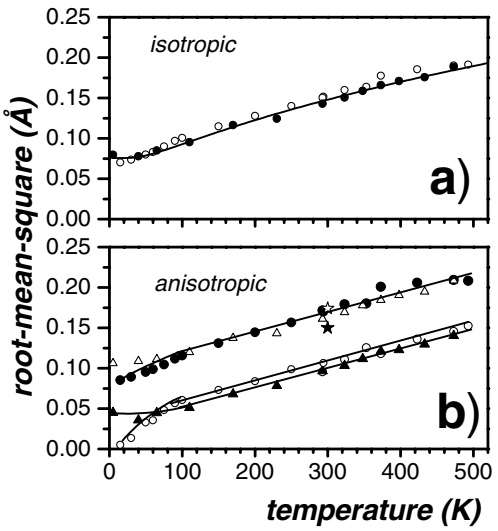

Fig. 6. (a) Isotropic root-mean-square displacement versus temperature for confined Se (open circles) and the bulk Se (solid circles). Solid line is a fit by the Einstein law. (b) Anisotropic root-mean-square displacement versus temperature: in the basal plane for confined Se (solid circles) and for the bulk (open triangles); along the hexagonal axis c for confined Se (open circles) and for the bulk (solid triangles). By the open and solid stars the rms amplitudes in the basal plane and along the hexagonal axis, respectively, from a single crystal experiments are shown [2]. The error is about the size of the symbols. Lines are the guide for the eye.

F(x) — Debye function:

$$F(x) = \frac{1}{x} \int_0^x \frac{y dy}{e^y - 1} \qquad (4)$$

leads to the Debye characteristic temperature Θ_D of 315(10) K, which is much more than of 135 K — the value of Θ_D reported for the bulk [21]. Taking into refinement the temperature independent constant as a refinable parameter does not improve the quality of convergence (goodness-of-fit). The static constant appears to be of 0.04(1) Å and $\Theta_D = 165(5)$ K.

Much better results can be obtained using the Einstein model of the independent vibrational modes [16]:

$$\langle u^2 \rangle = \frac{3\hbar^2}{m k_B \Theta_E} \left[\frac{1}{\exp(\Theta_E/T) - 1} + \frac{1}{2} \right]. \qquad (5)$$

A fit in the frame of the Einstein model with the only refined parameter Θ_E, the characteristic Einstein temperature, gives twice better convergence (goodness-of-fit) (solid line in Fig. 6a). The refined value of Θ_E appears of 161(5) K.

As expected the anisotropic rms amplitudes of atomic motion (Fig. 6b) appears to be essentially different in a basal plane and in the perpendicular direction, along the hexagonal c axis. These data are consistent with the early single crystal measurements of rms amplitudes in Se [2] shown for comparison in Figure 6.

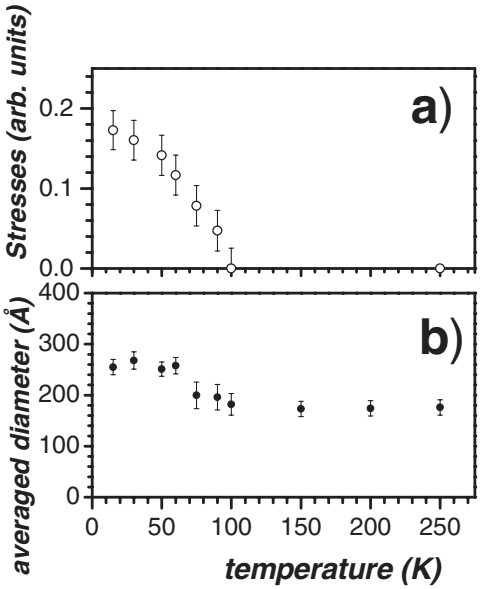

Fig. 7. Temperature dependencies of the inner stresses (a) and the volume averaged nanoparticle size (b).

The atomic motion anisotropy is intrinsic phenomenon and is observed in the nanostructured as well as in the bulk Se. It reflects the high anisotropy of the crystal structure of the trigonal Se, consisted of the weakly coupled rigid helix chains along the *c*-axis (Fig. 1). Indeed, the interaction between Se atoms within the spiral chains along hexagonal axis are much stronger than interaction between the chains. Therefore the rms amplitude in the basal plane, corresponding to the interaction between the chains is larger than in the perpendicular direction.

In Figure 6 it is seen that the atomic motion amplitudes in confinement are systematically slightly enhanced in contrast with the bulk above 100 K. There are the essential distinctions of the atomic motions at low temperatures. Especially the decrease of the motions is well-defined for the anisotropic root-mean-square displacements (Fig. 6b). It reflects the fundamental difference in the spectra of atomic motions in confinement and in the bulk.

It should note that in confined Pb [10] the situation is opposite: the atomic motions in confinement at low temperatures are stronger than those in the bulk. Apparently it is a result of the differences in the crystal structures of Pb and Se and different wetting ability, that leads to the different interaction of confined metals with a matrix.

In confinement we observe the surprising "freezing" of the atomic motion along the chains, while the atomic motion in the perpendicular plane (chain motion) still keeps (Fig. 6b). Moreover, it turns out that this "freezing" was accompanied by the appearance of the inner stresses and an increase of the volume averaged size of the confined nanoparticles (Fig. 7).

We did not detect any change of the background at low temperatures, i.e. there is no any crystallization of Se from the amorphous state, as it was observed at high temperatures. Therefore, the total volume of the embedded nanoparticles is constant. Since the observed slight increase of the averaged nanoparticle size means the change of a nanoparticle shape, which obviously becomes slightly elongated. Unfortunately because of a low statistical accuracy we cannot see it directly from the systematic peak broadening.

Note, that the unit cell of Se at low temperatures demonstrates the noticeable deformation (see Fig. 3), namely, with decreasing temperature the hexagonal prism length increases while the basal edge decreases. Obviously such deformation should favor the change of a nanoparticle shape.

There is no variation in the position of the diffuse peaks from a silica matrix. It means that the thermal expansion of the glass matrix is negligible in comparison with the thermal expansion of the embedded Se. Moreover, it is worth to remind that Se confined within nanopores crystallizes in the adjacent pores in the form of agglomerates rather than isotropic nanoparticles. As a result, the deformation of the nanoparticles "locked" in the silica matrix cavities causes the inner stresses.

Obviously due to the "locking" of the embedded Se within the matrix cavities the interaction with the cavity walls leads to a significant modification of the atomic motion in the confined nanoparticles. Therefore we attribute the observed "freezing" of the thermal vibration in the confined nanoparticles to this specific effect.

4 Conclusion

Neutron diffraction experiments demonstrated the presence of nanostructured Se confined within a porous glass matrix in a crystalline as well as in an amorphous state. The spontaneous partial crystallization of the crystalline Se from the confined amorphous phase was observed, which undergoes a maximum at about 150 °C before the melting.

The temperature dependence of the Debye-Waller parameters of the bulk Se can be well described by the Einstein formula for independent vibrations. The root-mean-square of the atomic motions are found essentially different in a base plane and in the perpendicular direction along the hexagonal axis in the bulk as well as in confinement due to strong crystal anisotropy.

The atomic motions in the confined Se differ from the atomic motions in the bulk at low temperatures, that reflects the fundamental difference in the spectra of the atomic vibrations in confinement and in the bulk.

The atomic motions in the confinement shows an unusual "freezing" along the chains, while the motion in the perpendicular plane still keeps. This "freezing" is accompanied by the deformation of the confined nanoparticles and the appearing the inner stresses. The last effect we attribute to the interaction of the confined nanoparticles with the cavity walls, which modifies the atomic motions.

The work was supported by the Grants: RFBR-06-02-17313, INTAS-2001-0826 and the program RAS "Effect of Atomic-Crystalline and Electronic Structure on the Properties of Condensed Matter". One of us I.V.G. acknowledges the financial support of NFL (Studsvik, Sweden).

References

1. *Pearson's handbook of crystallographic data for intermetallic phases* (ASM, Metals Park, Ohio, 1985)
2. P. Cherin, P. Unger, Inorganic Chemistry **6**, 1589 (1967)
3. K.E. Murphy, M.B. Altman, B. Wunderlich, J. Appl. Phys. **48**, 4122 (1977)
4. H.Y. Zhang, Z.Q. Hu, K. Lu, NanoStruct. Mat. **5**, 41 (1995)
5. Y.H. Zhao, K. Zhang, K. Lu, Phys. Rev. B **56**, 14322 (1997)
6. Y.H. Zhao, K. Lu, Phys. Rev. B **56**, 14330 (1997)
7. P. Armand, M.-L. Saboungi, D.L. Price, L. Iton, C. Cramer, M. Grimsditch, Phys. Rev. Lett. **79**, 2061 (1997)
8. I.L. Li, Z.K. Tang, J. Appl. Phys. **95**, 6364 (2004)
9. K. Matsuishi, K. Nogi, J. Ohmori, S. Onari, T. Arai, Z. Phys. D: At., Mol. Clusters **40**, 530 (1997)
10. I.V. Golosovsky, R.G. Delaplane, A.A. Naberezhnov, Y.A. Kumzerov, Phys. Rev. B **69**, 132301 (2004)
11. P. Levitz, G. Ehret, S.K. Sinha, J.M. Drake, J. Chem. Phys. **95**, 6151 (1991)
12. C. Kittel, *Introduction to Solid State Physics* (J. Wiley and Sons, Inc. NY, 1978)
13. B. Günther, O. Kanert, Phys. Rev. B **31**, 20 (1985)
14. A. Wannberg, A. Mellergard, P. Zetterstrom, R. Delaplane, M. Gronros, L. Karlsson, R. McGreevy, J. Neutron Research **8**, 133 (1999)
15. J. Rodriguez-Carvajal, Physica B **192**, 55 (1993); a recent version of Fullprof available at `http://journals.iucr.org/iucr-top/comm/cpd/newsletters`
16. B.T. Willis, A.W. Pryor, *Thermal Vibration in Crystallography* (Cambridge University Press, 1974)
17. P. Thompson, D. Cox, B. Hastings, J. Appl. Cryst. **20**, 79 (1987)
18. I.V. Golosovsky, I. Mirebeau, G. André, D.A. Kurdyukov, Yu.A. Kumzerov, S.B. Vakhrushev, Phys. Rev. Lett. **86**, 5783 (2001)
19. P. Jóvári, R.G. Delaplane, László Pusztai, Phys. Rev. B **67**, 172201 (2003)
20. F.G. Shi, J. Mater. Res. **9**, 1307 (1994)
21. *Internation Tables for X-ray Crystallography* (The Kynoch Press, Birmingham, 1962)